Construction and Building Materials 93 (2015) 884–890

Contents lists available at ScienceDirect

Construction and Building Materials

journal homepage: www.elsevier.com/locate/conbuildmat

Corrosion behavior of Cr modified HRB400 steel rebar in simulated concrete pore solution

Ming Liu, Xuequn Cheng, Xiaogang Li *, Zhu Jin, Haixia Liu

Corrosion and Protection Center, University of Science and Technology Beijing, Beijing 100083, China

HIGHLIGHTS

- New Cr modified steels resistant to corrosion are developed for steel rebar.
- Cr modified steels exhibit higher chloride thresholds and lower corrosion rates.
- Passive film of Cr modified steel and HRB400 steel are different.
- Cr modified steels have longer durability than HRB400 steel.

ARTICLE INFO

Article history:
Received 18 December 2014
Received in revised form 1 April 2015
Accepted 1 May 2015
Available online 16 May 2015

Keywords:
Alloy
Steel
EIS
Critical chloride level
Passive film

ABSTRACT

Cr modified alloy steels using HRB400 steel as base alloy were produced by remelting in a vacuum. Their corrosion resistance were estimated by open circuit potential, electrochemical impedance spectroscopy, X-ray photoelectron spectroscopy and immersion test in saturated $Ca(OH)_2$ simulated concrete pore solution. The modified alloy steels exhibit higher corrosion resistance with a high chloride thresholds, lower corrosion current density and higher impedance than HRB400 steel rebar. Cr can modify the proportion of Cr element in the passive film. The immersion test showed that the new alloy steels have lower corrosion rates. The new alloy steels have longer durability than HRB400 steel.

1. Introduction

At present, a large number of reinforced concrete structures are used in the marine environment. Reinforced concrete structure damage caused by chloride corrosion is widespread and causes great loses in economy [1–3]. In order to improve the durability of the concrete structure, the scholars and engineers have done a lot of research [4–8]. There are currently numerous strategies available for increasing the service life of reinforced structures exposed to chloride salts, including the use of: high performance concrete; chemical corrosion inhibitors, protective coatings on steel reinforcement, corrosion resistant steel, non-ferrous reinforcement, waterproofing membranes of sealants applied to the exposed surface of the concrete, cathodic protection, and combinations of the above. Concrete is a kind of permeable pore grid structure material and the concrete structure surface cracks can hardly be avoided, so in chloride enriched environment, it is inevitable for chloride ion penetration in concrete.

Some countries have already started to use stainless steel rebar in severe corrosive environment conditions [9–12]. Compared to carbon steel, stainless steel can significantly improve the chloride thresholds (CTL), prolongs the corrosion initial stage of rebar in concrete. In some corrosive environments, important and long service life designed new bridge structures using stainless steel showed significant corrosion resistance [10]. However, because it contains a large amount of expensive Cr and Ni element, the price of stainless steel is 4–6 times of carbon steel, limiting it widely use in project.

The corrosion resistance of steels to corrosive environments can be improved by adding alloy elements, which possibly differ in various corrosive environments. In the atmosphere, Cr, Cu and P in weathering steels are the main additives to increase resistance to electrochemical dissolution [13–15]. In a marine environment, Cr, Al and Mo in low-alloy steels have been considered as better than C steels [16–20]. In electrolytic solutions, the corrosion behavior of low-alloy steels with small amounts of Cr, Cu, Ni and Ca can be

* Corresponding author. Tel.: +86 15011217823; fax: +86 62334005.
E-mail address: lixiaogang@ustb.edu.cn (X. Li).

http://dx.doi.org/10.1016/j.conbuildmat.2015.05.073
0950-0618/

improved [21]. In order to improve the corrosion resistance of steel bar, Doctor Gareth Thomas invented a low carbon steel containing 9–11% Cr called MMFX steel rebar [22]. Independent tests show that MMFX provides twice the strength of conventional steel. It also provides five times more corrosion resistance than conventional steel and is superior to products such as epoxy-coated rebar (ECR) and galvanized rebar [10].

The mechanism of enhanced corrosion resistance is associated with Cr alloying. Protective corrosion products can form on the surface of low-Cr steel to improve CO_2 corrosion resistance [23]. A critical Cr content is set for low-alloy steels to avoid localized corrosion. The critical value ranges from more than 3 wt.% Cr to 4 wt.% Cr [24]. However, atmospheric environment and marine environment is generally neutral corrosion environment, the carbon dioxide dissolved in water is acidic corrosion system. Reinforcing steel in concrete is normally under a passive state due to the formation of a protective oxide layer on the steel surface, the corrosion mechanism is different from neutral and acidic corrosion systems [25–29].

Currently, carbon steel is still the dominant rebar in concrete structures. In marine environment, the corrosion resistance of carbon steel is very limited, adding small amount of Cr may improve the corrosion resistance of reinforced concrete in marine environment, also it cost will be reduced. However, there is little study on the corrosion behaviors of low Cr modified steel rebar in concrete.

In the present study, the effects of Cr on the corrosion behavior of carbon steel rebar are investigated. Using HRB400 steel rebar as base material, Cr modified steels were produced by remelting in a vacuum. The electrochemical corrosion behavior of the modified steels is estimated by open circuit potential and electrochemical impedance spectroscopy (EIS) in saturated $Ca(OH)_2$ concrete pore solution containing various concentrations of chloride ions. The chloride thresholds of the Cr modified steels were compared with HRB400 steel rebar, the corrosion kinetics of the modified steels was compared with HRB400 steel.

2. Experimental

2.1. Materials and solution

The steel used was HRB400 steel rebar made by China Nanjing iron and Steel Group Company. The chemical composition (in % by mass) was 0.19% C, 0.57% Si, 0.57% Mn, 0.024% S, 0.017% P and the residual Fe. Two alloy steels were prepared by adding 1.5 wt.% Cr, 3.0 wt.% Cr and 5.0 wt.% Cr to HRB400 steel bases. The steels were then remelted in a vacuum induction furnace. The new alloy steels were respectively marked as Steels 1.5Cr, 3Cr and 5Cr. The steel samples were reheated at 1200 °C for 30 min and rolled to approximately 50% thickness reduction. Plates that were 4 mm thick were obtained. The plates were reheated at 900 °C for 10 min and cooled in air. The microstructures observed via optical microscopy consisted of ferrite-pearlite which was the same as the as-received HRB400 steel.

The modified steels and HRB400 steel were machined into specimens for electrochemical measurements and immersion tests. The specimens for the electrochemical measurements had a dimension of 10 × mm10 × mm × 3 mm, whereas those for the immersion tests had a dimension of 50 mm × 25 mm × 3 mm The exposed surface of the specimens for electrochemical measurements was 10 mm × 10 mm, with an area of 1 cm^2. A copper wire was welded to one end surface of the steel specimen and the other end surface was used to test in the electrochemical methods. The flank and the end surface with a thick copper wire were sealed by means of epoxy resin. The tested surface was polished with SiC water polishing papers with grits of 150#, 400#, 800#, 1000# and 1200#. Last, the steel specimen was ultrasonically degreased in acetone and washed in distilled water.

The saturated $Ca(OH)_2$ solution was chosen to simulate the concrete pore solution in the present work. All chemical reagents applied in the current work were of analytical grade reagents and experimental water was deionized water.

2.2. Electrochemical measurements

The electrochemical measurements were carried out with the Partstat 2273 Advanced Potentiostat/Galvanostat/FRA system. A classical 3-electrode device system was employed: the steel bar was a working electrode, while a saturated calomel electrode and a platinum electrode were connected to work as a reference and auxiliary electrode, respectively.

Prior to the measurements, the steel bars were immersed in the saturated $Ca(OH)_2$ solution for 7 days to promote a passive layer in order to simulate field condition sand three parallel steel samples were placed in every exposure solution [30,31]. After this, the aggressive chloride ions were supplied by sodium chloride and added 0.2 wt.% every 2 days, the E_{corr} and EIS were measured at the end of the 2-day period. The EIS data was obtained with the frequency range from 100 kHz to 10 mHz and a sinusoidal potential perturbation of 10 mV at the open circuit potentials. The experimental results were interpreted based on an equivalent electrical circuit by using a suitable fitting procedure of ZSimpWin. All measurements were carried out at ambient temperature approximately 25 °C.

2.3. XPS analysis

The chemical composition of the films was investigated by X-ray photoelectron spectrometer (XPS) with a monochromatic Al K_a radiation source and a hemispherical electron analyzer operating at a pass energy of 25 eV. The curve fitting was performed by the commercial software Xpspeak version 4.1, which contained the Shirley background subtraction and Gaussian–Lorentzian tail function for better spectra fitting.

2.4. Immersion test

Immersion test was conducted in saturated $Ca(OH)_2$ solution with 10 wt.% NaCl solution at 35 °C. The 10% of NaCl (wt.%) was added into the solution to accelerate the corrosion process, and simultaneously to simulate the very aggressive environment such as salt mines or the structures used in the splash zones [32,33]. After the test, the morphology of the corroded specimens was observed, and the corrosion rates were obtained through the weight loss of the specimen.

3. Results and discussion

3.1. Evolution of electrode potentials

The evolutions of the E_{corr} for the specimens immersed in saturated $Ca(OH)_2$ solution with the concentrations of chloride ions are presented in Fig. 1. It can be found that, the E_{corr} for the specimens without chloride ions are around −250 mV vs. SCE. With the increasing amount of chloride ions, the E_{corr} gradually reduce. Moreover, an abrupt decrease for E_{corr} appears when the chloride ions are reached a certain level, which is due to the breakdown of the passive film caused by the aggressive chloride ions. And it is suggested that the E_{corr} ranges from −350 mV to −450 mV at the corrosion initiation [31], Fig. 2 shows the critical chloride level (CTL) of steels. The CTL in saturated $Ca(OH)_2$ solution were 2.8 wt.% NaCl for 1.5Cr steel, 4.4 wt.% NaCl for 3Cr steel and 7.4 wt.% NaCl for 5Cr Steel which are more large than the value of 1.2 wt.% NaCl for HRB400 steel. The phenomenon indicates that adding Cr in HRB400 steel can significantly improve the chloride thresholds of the steel rebar. This finding is consistent with some research on MMFX steel [27].

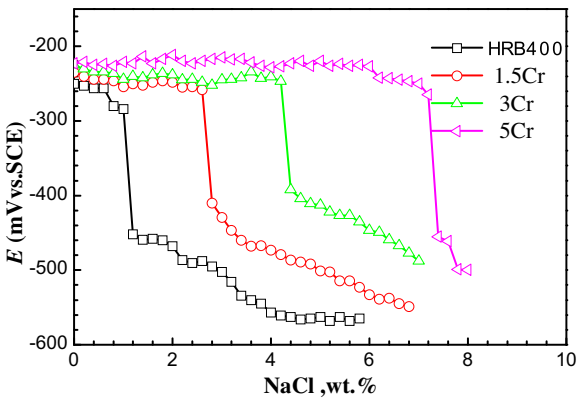

Fig. 1. Variations of the E_{corr} for the specimens in saturated $Ca(OH)_2$ solution with different concentrations of chloride ions.

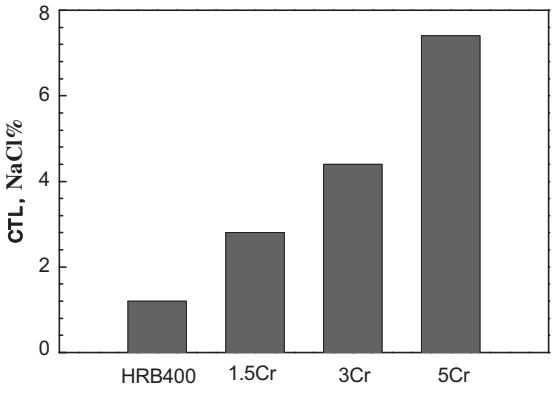

Fig. 2. CTL of the specimens in saturated $Ca(OH)_2$ solution.

3.2. EIS

The Nyquist plots of EIS immersed in saturated $Ca(OH)_2$ solution with different concentrations of chloride ions is given in Fig. 3. Nyquist plots usually show a capacitive loop and the diameter of capacitive loops decrease with the increase of chloride ions, which is caused by the corrosion of chloride ions on the oxide layer of the steel surface. Electrochemically, the EIS curve in the high frequency suggests the resistance between electrolyte solution and the working electrode while that in the low frequency is closely related to the charge transfer resistance of the corrosion process [34]. An equivalent electrical circuit with one time constants, as shown in Fig. 4, is proposed to simulate the electrochemical process of steels which has been used by other authors [35]. In Fig. 4, R_s is the resistance of the solution, R_p represents the polarization resistance caused by charge transfer reaction. R_p consists of passive film resistance R_f and charge transfer resistance R_{ct} [36]. The protective performance of passive film can thus be described by R_p. Q_{dl} is a constant phase element (CPE) or a capacitance of the double layer capacitor that characterizes the charge separation between the metal and electrolyte interface. The total impedance Z, shown in Fig. 4, can be written as:

$$Z = R_s + \frac{1}{Z_{Q_{dl}} + \frac{1}{R_p}} \tag{1}$$

However, the double-layer capacitor does not behave ideally because of the roughness caused by the corrosion product layer. The impedance of a capacitor has the following form [37]:

$$Z_{Q_{dl}}^{-1} = Q_{dl}(j\omega)^n \tag{2}$$

where ω is the angular frequency, j is the imaginary number and n is the CPE power. The factor n is typically between 0.5 and 1.0 [38]. When $n = 1$, a CPE is equivalent to an ideal capacitor.

The impedance of Q_f has the same form as that of Q_{dl} in Eq. (1).

The values of the electrical circuit elements from the best fitting are listed in Tables 1–4. It can be seen that Cr modified steel have higher R_p than HRB400 steel. This result indicates that adding Cr in steel is advantageous for corrosion resistance. R_p was introduced into the Stern–Geary equation to calculate the corrosion current density (I_{corr}). The Stern–Geary equation is $I_{corr} = B/R_p$; in which B is Stern–Geary constant, assumed to be 26 mV [39,40].

The I_{corr} obtained from the EIS curves for the specimens immersed in saturated $Ca(OH)_2$ solution with the concentrations

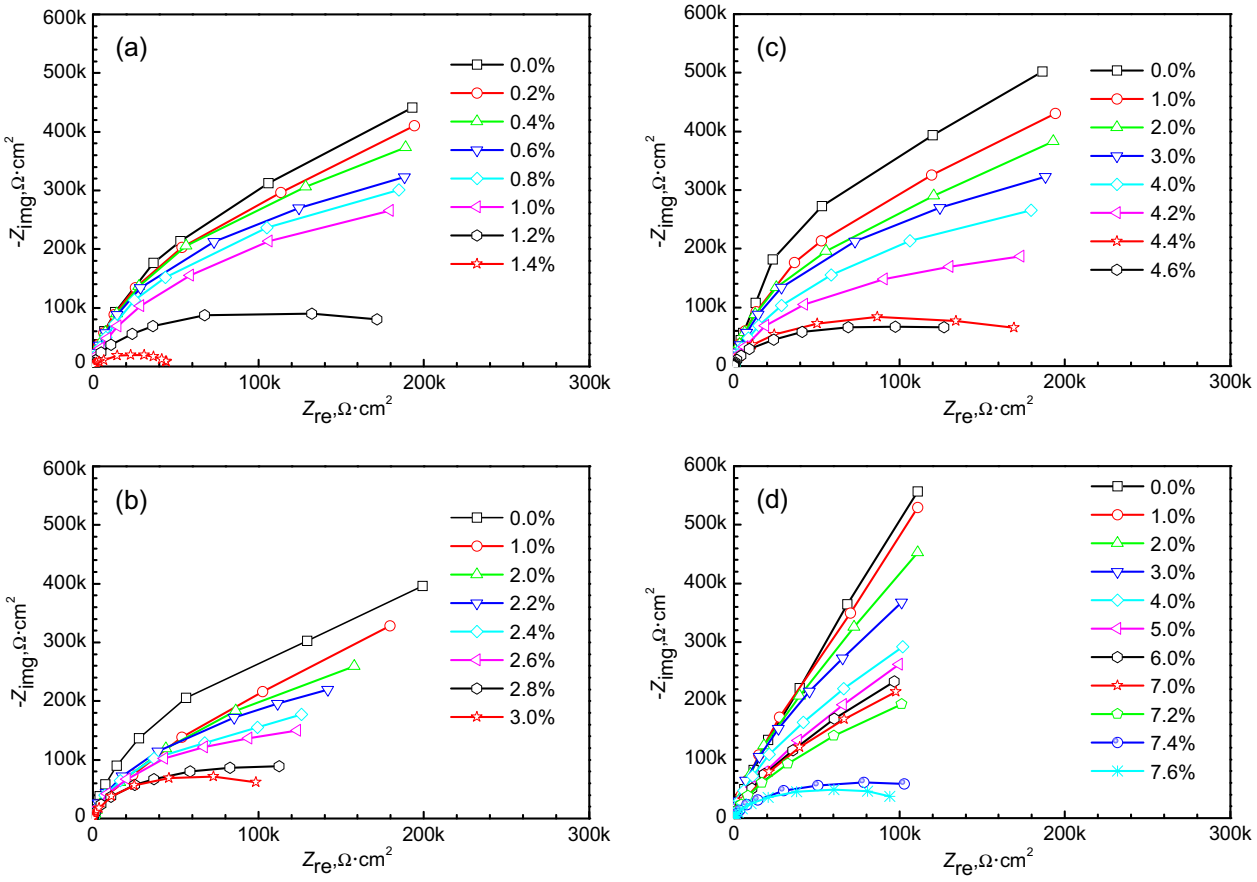

Fig. 3. Nyquist plots for the specimens in saturated $Ca(OH)_2$ solution containing various concentrations of chloride ions. (a) HRB400, (b) 1.5Cr, (c) 3Cr, (d) 5Cr.

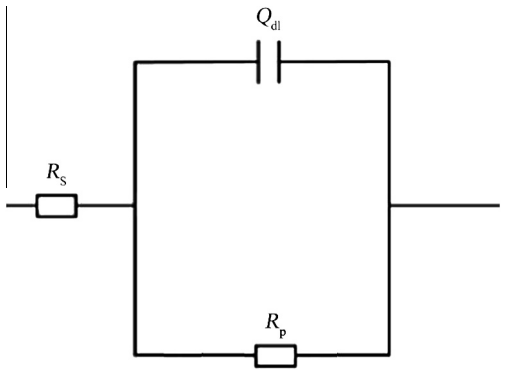

Fig. 4. Equivalent circuit applied to analyze the measured EIS results.

Table 1
EIS fitting parameter values of HRB400 steel rebar.

NaCl (wt.%)	R_s, Ω·cm²	Q_{dl}, μF·cm^{-2}·S^{n-1}	n	R_p, kΩ·cm²
0	17.34	0.274	0.96	867
0.2	16.98	0.269	0.96	839
0.4	16.73	0.266	0.95	813
0.6	15.57	0.316	0.94	765
0.8	14.02	0.263	0.96	578
1.0	11.46	0.324	0.94	400
1.2	11.36	0.281	0.96	236
1.4	10.13	0.404	0.93	186

Table 2
EIS fitting parameter values of 1.5Cr steel rebar.

NaCl (wt.%)	R_s, Ω·cm²	Q_{dl}, μF·cm^{-2}·S^{n-1}	n	R_p, kΩ·cm²
0	17.28	0.269	0.97	963
1	11.62	0.234	0.97	618
2	7.90	0.346	0.96	508
2.2	7.87	0.317	0.95	476
2.4	7.75	0.342	0.96	424
2.6	7.62	0.358	0.95	348
2.8	7.36	0.413	0.94	211
3.0	7.43	0.466	0.93	161

Table 3
EIS fitting parameter values of 3Cr steel rebar.

NaCl (wt.%)	R_s, Ω·cm²	Q_{dl}, μF·cm^{-2}·S^{n-1}	n	R_p, kΩ·cm²
0	17.48	0.255	0.96	1083
1	11.38	0.281	0.96	605
2	7.90	0.350	0.98	531
3	7.52	0.301	0.95	500
4	6.61	0.268	0.97	390
4.2	5.30	0.264	0.97	317
4.4	5.27	0.294	0.96	228
4.6	4.96	0.281	0.97	207

of chloride ions are depicted in Fig. 5. Initially, the corrosion current densities I_{corr} are quite low because of the compact oxide layer on the steel surface. With the chloride ions increase, the I_{corr} increase gradually and a sharp increase for I_{corr} occurs when a certain level of chloride ions is reached. Similar to the abrupt change of E_{corr}, the abrupt increase of I_{corr} is associated with the damage of the passive film, indicating that the active corrosion of pitting occurs. So, the CTL for the HRB400 is 1.2 wt.% NaCl, 4.4 wt.% NaCl for 3Cr steel and 7.4 wt.% NaCl for 5Cr steel. In addition, the I_{corr} for the specimens at the onset of pitting corrosion is more than

Table 4
EIS fitting parameter values of 5Cr steel rebar.

NaCl (wt.%)	R_s, Ω·cm²	Q_{dl}, μF·cm^{-2}·S^{n-1}	n	R_p, kΩ·cm²
0	16.89	0.449	0.90	3250
1	13.29	0.445	0.94	1529
2	13.59	0.437	0.91	1238
3	13.09	0.442	0.92	1130
4	10.65	0.332	0.94	1000
5	5.91	0.386	0.93	800
6	4.59	0.279	0.96	600
7	4.13	0.217	0.95	400
7.2	3.71	0.240	0.95	310
7.4	3.28	0.466	0.84	170
7.6	2.76	0.789	0.83	146

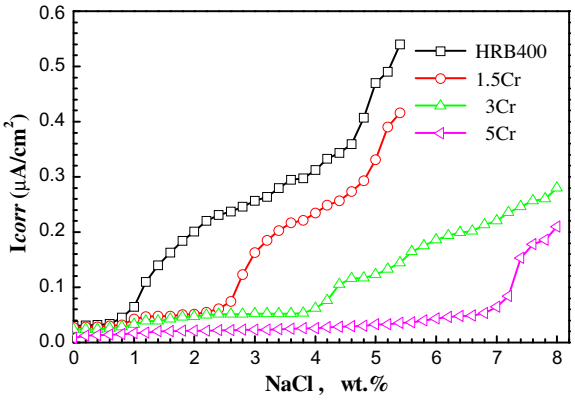

Fig. 5. Variations of the I_{corr} for the specimens in saturated $Ca(OH)_2$ solution containing various concentrations of chloride ions.

0.1 μA/cm², which is usually regarded as the sign of active corrosion for the steel in some previous literatures [39,41]. It can be seen that with the increase of Cr content, the CTL value of steels are increased. The chloride threshold value of 1.5Cr, 3Cr, 5Cr steel is 2.3, 3.7, 6.2 times larger than HRB400 carbon steel. Cr alloy can significantly improve the durability of HRB400 carbon steel rebar in marine environment.

3.3. Composition of passive film

The chemical composition of the passive film may have great impacts on the semiconducting properties and corrosion behavior of steel. The chemical composition of the passive film formed at OCP in saturated $Ca(OH)_2$ solution for 7 day was assessed by XPS. As shown in Figs. 6–8, all of the metallic and oxidized states of Fe2p3/2, Cr2p3/2, O1s, are presented. After background subtraction according to Shirley, the XPS results are separated into contributions of the different oxidation states by a fit procedure. Binding energy shift was observed mainly in iron (Fe2p3/2), chromium (Cr2p3/2), oxygen (O1s), profiles indicating changes in passive film composition with increase in chromium content. Spectra deconvolution of the primary compounds of the passive film, such as iron, chromium, oxygen, are shown based on their binding energies (E_b), which are listed in Table 5.

As is shown in the Fig. 6, the iron profile showed mainly three peaks Fe (met) (707.7 eV), FeO (709.4 eV) and FeOOH (711.8 eV). Compared with the relative peak heights of Fe^{2+} and Fe^{3+} indicate that FeOOH are the primary iron oxidized species in the passive film of HRB400, 1.5Cr, 3Cr and 5Cr steel in the saturated $Ca(OH)_2$ solution.

As is shown in the Fig. 7, the chromium peaks could only be seen in 3Cr and 5Cr steel, and the chromium profile showed mainly two peaks: $Cr(OH)_3$ (577.1 eV) and CrO_3(578.2 eV). As the content

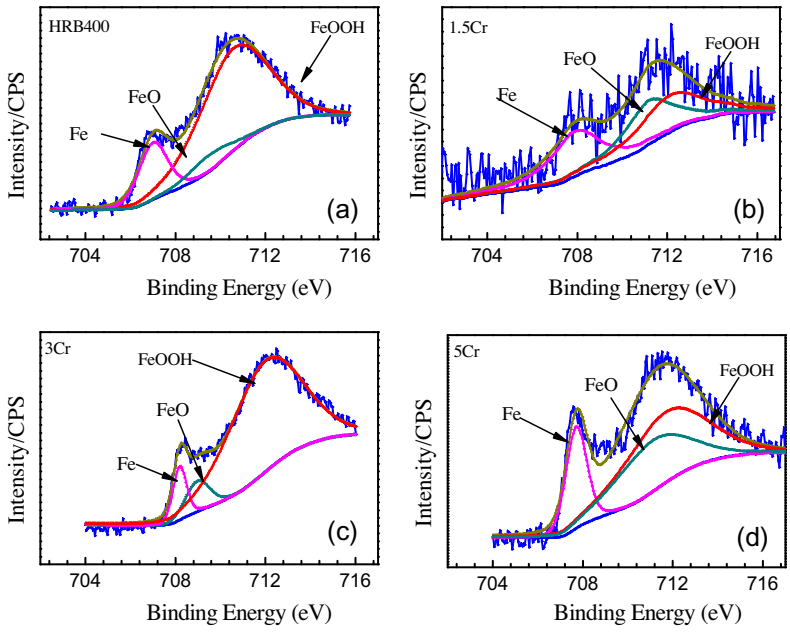

Fig. 6. The XPS spectra of Fe2p3/2 of the passive films formed on steel surface after passivation in saturated $Ca(OH)_2$ solution for 7 days.

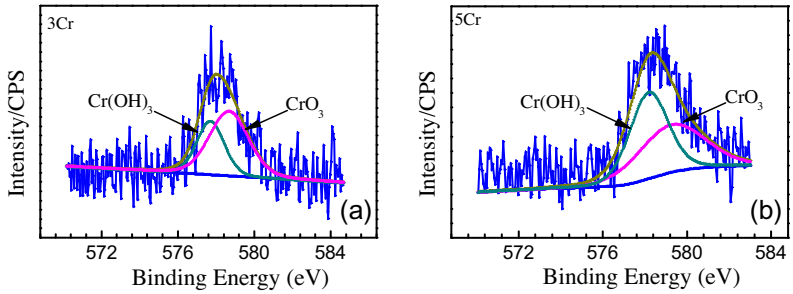

Fig. 7. The XPS spectra of Cr2p3/2 of the passive films formed on steel surface after passivation in saturated $Ca(OH)_2$ solution for 7 days.

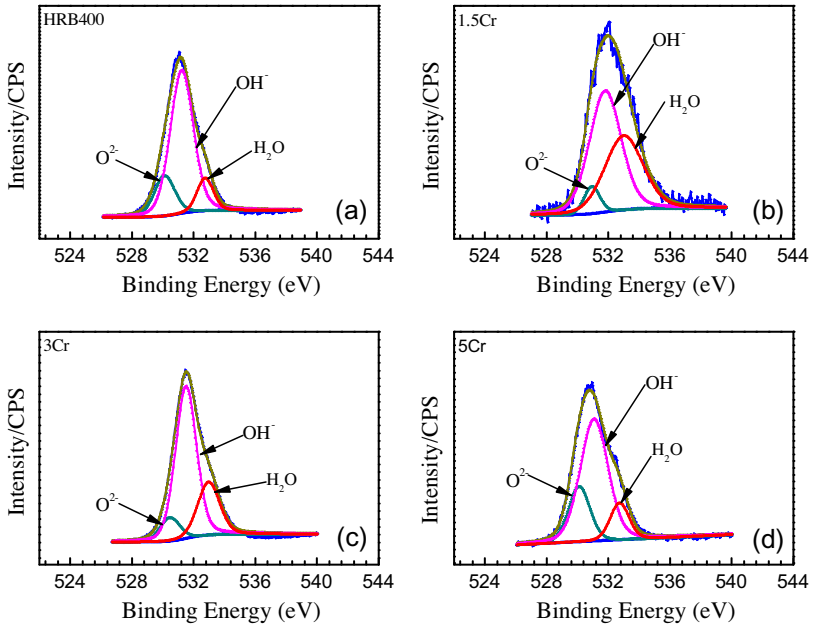

Fig. 8. The XPS spectra of O1s of the passive films formed on steel surface after passivation in saturated $Ca(OH)_2$ solution for 7 days.

Table 5
The binding energies of the primary compounds of steel passive film obtained from XPS spectra deconvolution.

Element	Peak	Species/bing energy (eV)
Fe	$2p_{3/2}$	Fe(met)/707.7; FeO/709.4; FeOOH/711.8
O	1S	O^{2-}/530.2; OH^-/531.8; H_2O/533
Cr	$2p_{3/2}$	$Cr(OH)_3$/577.1; CrO_3/578.2

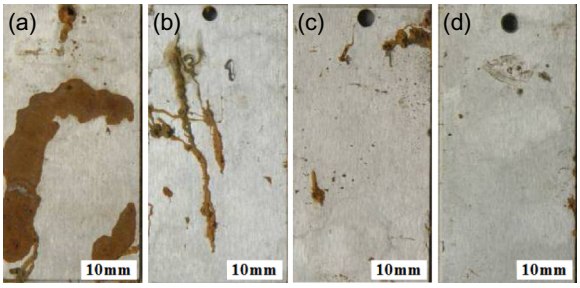

Fig. 9. Corrosion morphology of steel immersion in saturated $Ca(OH)_2$ solution with 10% NaCl for 7 days. (a) HRB400, (b) 1.5Cr, (c) 3Cr, (d) 5Cr.

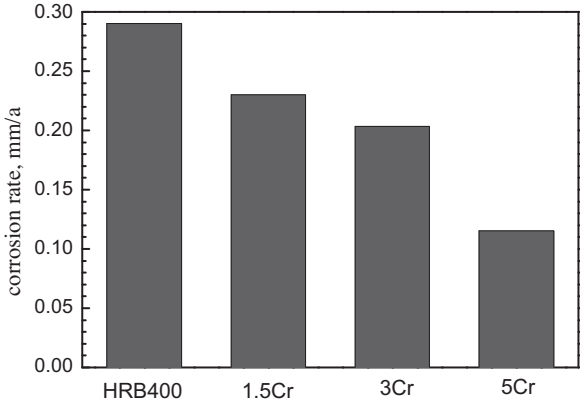

Fig. 10. The corrosion rate of steel immersion in saturated $Ca(OH)_2$ solution with 10% NaCl for 7 days.

of the chromium increased, the intensity of CrO_3 is less compared to the 3Cr steel and the intensity of $Cr(OH)_3$ is much higher. Hence, in saturated $Ca(OH)_2$ solution, the addition of chromium to the HRB400 steel may change the components of the passive film [42].

Fig. 8 also shows the core-level spectra of the passive film formed on steel rebar in the O1s region. Oxygen species, O^{2-} and OH^-, in passive film play the role of connecting metal ions. The O1s spectra may also be split into three components O^{2-} (530.2 eV), OH^- (531.8 eV) and H_2O (533 eV). It can be seen that OH^- is the primary constituent of the passive film, which corresponds to the formation of $Cr(OH)_3$ and FeOOH. While O^{2-} is also the primary constituent of the passive film, which corresponds to the formation of FeO.

3.4. Corrosion rates from the immersion test

According to some research results, weight loss method in simulated concrete pore solution could reflect the steel rebar corrosion behavior in concrete [43,44]. To simulate the corrosion behavior of extremely harsh environment, immersion test were performed on the steel specimens in saturated $Ca(OH)_2$ solution with 10 wt.% NaCl solution for 7 days. After the immersion test, the surfaces of the corroded specimens were observed. The corrosion rates were obtained by the weight loss of the specimens. The images of the steel specimens immersed in saturated $Ca(OH)_2$ solution with 10 wt.% NaCl solution at 35 °C for 7 d are shown in Fig. 9. Localized corrosion occurs on the specimens of steels. HRB400 steel surface has a lot of corrosion products, with the increase of Cr element content, steel corrosion degree decreased significantly.

The average corrosion rates from the weight loss of the specimen are shown in Fig. 10. Cr modified steel have lower corrosion rates than HRB400 steel, thus indicating that Cr element in steel improve corrosion resistance. 5Cr steel has the lowest corrosion rate, its corrosion rate is only 39.8% of HRB400 steel. From the results of immersing corrosion test, corrosion rate of Cr modified steel was significantly lower than that of HRB400 steel, which means once the steel rebar start to corrosion in concrete, using Cr modified steels could prolong the time of concrete cracking.

4. Conclusions

In this paper, the results obtained from the present study on the effects of Cr on the corrosion behavior of steel in saturated $Ca(OH)_2$ simulated concrete pore solution have been presented. The following conclusions can be drawn from this investigation:

(1) Cr modified steels exhibit higher corrosion resistance with a higher chloride threshold value. Cr modified steels have a lower corrosion current density and higher impedance than HRB400 steel. The chloride thresholds value of 1.5Cr, 3Cr, 5Cr steel is 2.3, 3.7, 6.2 times larger than HRB400 steel.
(2) It can be concluded that the primary constituents of the films in saturated $Ca(OH)_2$ simulated concrete pore solution are iron oxides. With the increase of the content of Cr element, chromium oxides can be observed in 3Cr and 5Cr steel passive film.
(3) Compared with HRB400 steel rebar, with the Cr element content increased, the corrosion rate decreased, 5Cr steel has the best corrosion resistance.

Acknowledgments

This work was supported by the National Basic Research Program of China (973 Program project, No. 2014CB643300) and the National Science and Technology Infrastructure Platforms Construction Project.

References

[1] Du YL, Shi ZM. The state of art on corrosion and prevention of reinforced concrete. J Jilin Inst Technol 1998;19(2):1–8.
[2] Sheng DJ, Wu SX. Experimental study and analysis on the mechanical performance of corroded reinforcement concrete beams in atmospheric environment. China Civil Eng J 2009;42(08):75–83.
[3] Mahdi V, Mohammad S, Pouria G. Comparative studies of experimental and numerical techniques in measurement of corrosion rate and time-to-corrosion-initiation of rebar in concrete in marine environments. Cement Concr Compos 2014;48:98–107.
[4] Gameiro F, Brito J, Silva D. Durability performance of structural concrete containing fine aggregates from waste generated by marble quarrying industry. Eng Struct 2014;59:654–62.
[5] Wen XD, Tu JL, Gan WZ. Durability protection of the functionally graded concrete in the structure splash zone. Constr Build Mater 2013;41:246–51.
[6] Antonios K, Michael FP, Ioannis I. Durability performance of self-compacting concrete. Constr Build Mater 2012;41:320–5.
[7] Moetaz ME, Ali AJ. Durability assessment of epoxy modified concrete. Constr Build Mater 2010;24(8):1523–8.
[8] Douglas HR, John AB. Design for durability: the key to improving concrete sustainability. Constr Build Mater 2014;67(Part C):422–30.
[9] Shi JJ, Sun W. Recent research on steel corrosion in concrete. J Chin Ceram Soc 2010;38(9):1753–64.
[10] Ge Y, Zhu XY, Li Y. Corrosion of reinforced concrete bridge structures. Chemical Industry Press; 2011.

[11] Criado M, Bastidas DM, Fajardo S, et al. Corrosion behaviour of a new low-nickel stainless steel embedded in activated fly ash mortars. Cement Concr Compos 2011;33(6):644–52.
[12] Abdulrahman A, Raja RH, Rajeh AZ, Abdulaziz AN. Corrosion of reinforcement in concrete construction. Constr Build Mater 2012;38(9):67–81.
[13] Yamashita M, Miyuki H, Matsuda Y, et al. The long term growth of the protective rust layer formed on weathering steel by atmospheric corrosion during a quarter of a century. Corros Sci 1994;36:283–99.
[14] Hao L, Zhang S, Dong J, et al. Evolution of corrosion of MnCuP weathering steel submitted to wet/dry cyclic tests in a simulated coastal atmosphere. Corros Sci 2012;58:175–80.
[15] Wang Z, Liu J, Wu L, et al. Study of the corrosion behavior of weathering steels in atmospheric environments. Corros Sci 2013;67:1–10.
[16] Huang Y, Su F. An electrochemical study of the corrosion resistance of 12Cr2MoAlXt alloy steel in sea water. J Chin Soc Corros 1988;8(1):72–7.
[17] Shifler DA. Understanding material interactions in marine environments to promote extended structural life. Corros Sci 2005;47:2335–52.
[18] Zhang P, Yu H. Microstructure and properties of seawater corrosion resistant steel 10CrMoAl. J Wuhan Univ Sci Technol 2010;33(2):176–9.
[19] Melchers RE. Effect of small compositional changes on marine immersion corrosion of low alloy steels. Corros Sci 2004;46:1669–91.
[20] Wang R, Luo SJ, Liu M, et al. Electrochemical corrosion performance of Cr and Al alloy steels using a J55 carbon steel as base alloy. Corros Sci 2014;85:270–9.
[21] Choi Y-S, Shim J-J, Kim J-G. Effects of Cr, Cu, Ni and Ca on the corrosion behavior of low carbon steel in synthetic tap water. J Alloy Compd 2005;391:162–9.
[22] De Rojas Ricardo R. New developments in steel protection from corrosion. Massachusetts: Institute of Technology; 2001.
[23] Ingham B, Ko M, Kear G, et al. In situ synchrotron X-ray diffraction study of surface scale formation during CO_2 corrosion of carbon steel at temperatures up to 90 °C. Corros Sci 2010;52:3052–61.
[24] Kamimura T, Stratmann M. The influence of chromium on the atmospheric corrosion of steel. Corros Sci 2001;43:429–47.
[25] Sagoe-Creutsil KK, Yilmaz VT, Glasser FP. Corrosion inhibition of steel in concrete by carboxylic acids. Cem Concr Res 1993;23:1380–8.
[26] Freire L, Novoa XR, Montemor M, et al. Study of passive films formed on mild steel in alkaline media by the application of anodic potentials. Mater Chem Phys 2009;114:962–72.
[27] Poursaee A. Corrosion of steel bars in saturated $Ca(OH)_2$ and concrete pore solution. Concr Res Lett 2010;1:90–7.
[28] Ghods P, Isgor OB, McRae G, Miller T. The effect of concrete pore solution composition on the quality of passive oxide films on black steel reinforcement. Cement Concr Compos 2009;31:2–11.
[29] Haleem SM, Wanees S, Bahgat A. Environmental factors affecting the corrosion behaviour of reinforcing steel. V. Role of chloride and sulphate ions in the corrosion of reinforcing steel in saturated $Ca(OH)_2$ solutions. Corros Sci 2013;75:1–15.
[30] Poursaee A, Hansson CM. Reinforcing steel passivation in mortar and pore solution. Cem Concr Res 2007;37(7):1127–33.
[31] Liu R, Jiang LH, Xu JX, et al. Influence of carbonation on chloride-induced reinforcement corrosion in simulated concrete pore solutions. Constr Build Mater 2014;56:16–20.
[32] Mangat PS, Limbachiya MC. Effect of initial curing on chloride diffusion in concrete repair materials 1999. Cem Concr Res 1999;29(9):1475–85.
[33] Freire L, Carmezima MJ, Ferreira MGS, et al. The electrochemical behaviour of stainless steel AISI 304 in alkaline solutions with different pH in the presence of chlorides. Electrochim Acta 2011;56:5280–9.
[34] Luo H, Dong CF, Li XG, et al. The electrochemical behavior of 2205 duplex stainless steel in alkaline solutions with different pH in the presence of chloride. Electrochim Acta 2012;64:211–20.
[35] Wei J, Dong JH, Ke W. Corrosion resistant performance of a chemical quenched rebar in concrete. Constr Build Mater 2011;25:1243–7.
[36] Mansfeld F. Electrochemical Impedance Spectroscopy (EIS) as a new tool for investigating methods of corrosion protection. Electrochim Acta 1990;35(10):1533–44.
[37] Macdonald JR. Impedance spectroscopy. Ann Biomed Eng 1992;20:289–305.
[38] Zhang X, Pehkonen SO, Kocherginsky N, et al. Copper corrosion in mildly alkaline water with the disinfectant monochloramine. Corros Sci 2002;44:2507–28.
[39] Montemor MF, Simões AMP, Ferreira MGS. Chloride-induced corrosion on reinforcing steel: from the fundamentals to the monitoring techniques. Cem Compos 2003;25(4–5):491–502.
[40] Ahmad S. Reinforcement corrosion in concrete structures, its monitoring and service life prediction – a review. Cem Compos 2003;25(4–5):459–71.
[41] Andrade C, Alonso C. Test methods for on-site corrosion rate measurement of steel reinforcement in concrete by means of the polarization resistance method. Mater Struct 2004;37(9):623–43.
[42] Luo H, Li XG, Dong CF, et al. The influence of Cu on the electrochemical behaviour of 304 stainless steel in 0.1M H_3PO_4 solution. Surf Interface Anal 2013;45:793–9.
[43] Tang YM, Zhang GD, Zuo Y. The inhibition effects of several inhibitors on rebar in acidified concrete pore solution. Constr Build Mater 2012;28:327–32.
[44] Valcarce MB, Lopez C, Vazquez M. The role of chloride, nitrite and carbonate ions on carbon steel passivity studied in simulating concrete pore solutions. J Electrochem 2012;159:244–51.